

# Theoretical Study of C–H and C–F Activation in CH<sub>4–n</sub>F<sub>n</sub> (n = 1–4) Molecules by Platinum

F. Colmenares\* and H. Torrens

División de Estudios de Posgrado, Facultad de Química, Universidad Nacional Autónoma de México, México D.F. 04510, Mexico

Received: June 2, 2005; In Final Form: September 14, 2005

CASSCF followed by MRMP2 calculations have been carried out to analyze the reactions of a naked platinum atom with the fluorocarbon compounds CH<sub>4–n</sub>F<sub>n</sub> (n = 1–4). For each of these interactions the potential-energy surfaces which correlate with the triplet ground state and the first excited singlet state of the free fragments were investigated for representative states evolving from different approaching modes of the reactants. For all the fluorinated fragments activation of the C–H and C–F bonds by the metal is strongly determined by the low-multiplicity channels arising from the first excited asymptote. Although stable products are predicted for insertion of the metallic atom into both the C–H and the C–F bonds of the different fluorocarbon compounds, comparison between the calculated energy barriers for reactions taking place in the same fluorinated molecule suggests in all cases a kinetic preference for the C–H bond oxidative addition to the platinum atom.

## 1. Introduction

Activation of the C–H bond by transition-metal-containing systems has received considerable attention both experimentally and theoretically due mainly to its catalytic relevance.<sup>1–8</sup> Recently, the study of reactions involving C–F bond activation has also emerged as an attractive research field.<sup>9–15</sup> In particular, intramolecular C–F activation occurring in different transition-metal-containing compounds has been investigated by several groups.<sup>16–18</sup> Competition between C–H and C–F bond activation reactions often occurs in these kinds of systems, the C–H activation products often being preferred in most of the cases.<sup>19</sup> Although experimental observations and theoretical studies suggest a kinetic origin for this preference,<sup>14</sup> conclusions in this sense have not been achieved.

The theoretical study of simple reactions such as those involving a naked transition-metal atom interacting with small fluorocarbon molecules could provide some insight into the electronic factors which determine the competition between the C–H and C–F bond activation reactions. In this line, Smurnyi et al.<sup>8</sup> reported results obtained through DFT calculations for interaction of a single platinum atom with the fluoromethane molecule. According to these authors the insertion reaction of the metallic atom into the C–H bond of the fluorinated molecule is thermodynamically favorable and occurs along an energy barrierless path. Interestingly, the corresponding C–F activation reaction is also exothermic, but it requires surmounting an energy barrier before the product of the oxidative addition could be attained.<sup>8</sup>

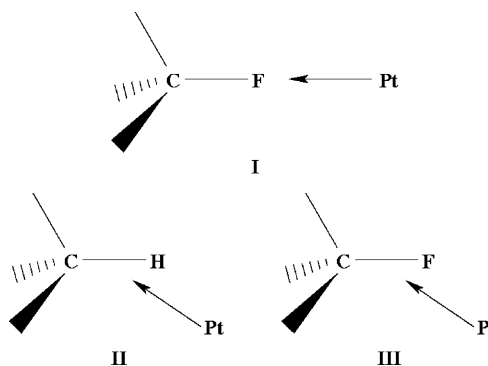
In this paper the low-lying electronic states evolving from interaction of a naked platinum atom with the fluorocarbon compounds CH<sub>4–n</sub>F<sub>n</sub> (n = 1–4) are determined for different approaching modes of the reactants. Likewise, reaction channels leading to C–H and C–F bond activation in the different fluorocarbon molecules are comparatively analyzed. Metal–halogen interactions arising at the initial stage of most of the investigated systems are also discussed as being important in

determining the competition between the C–H and C–F bond activation reactions.

## 2. Computational Details

Potential-energy surfaces were calculated at the CASSCF level for representative electronic states belonging to the C<sub>s</sub> symmetry group which evolve from the ground state, Pt(<sup>3</sup>D;5d<sup>9</sup>6s<sup>1</sup>) + CH<sub>4–n</sub>F<sub>n</sub>, and the first excited state, Pt(<sup>1</sup>S;5d<sup>10</sup>) + CH<sub>4–n</sub>F<sub>n</sub>, of the free fragments. Three different approaching modes of the reactants were taken into account. First, the C–F–Pt angle was kept fixed at 180°, thus favoring direct interaction between the fluorine and platinum atoms (I in Scheme 1).

SCHEME 1



Potential-energy curves for electronic states evolving from this approach were calculated performing geometry optimization calculations at selected Pt–F distances in the interval 2–6 Å. The two remaining approach modes of the reactants (II and III in Scheme 1) involved insertion of the metallic atom into the C–H and C–F bonds of the fluorinated fragments. For these insertion reactions potential-energy curves for the low-lying electronic states belonging to the C<sub>s</sub> symmetry group were obtained performing geometry optimization calculations each 10° between 0° and 180° for the H–Pt–C and F–Pt–C angles.

\* Corresponding author. E-mail: colmen@servidor.unam.mx.

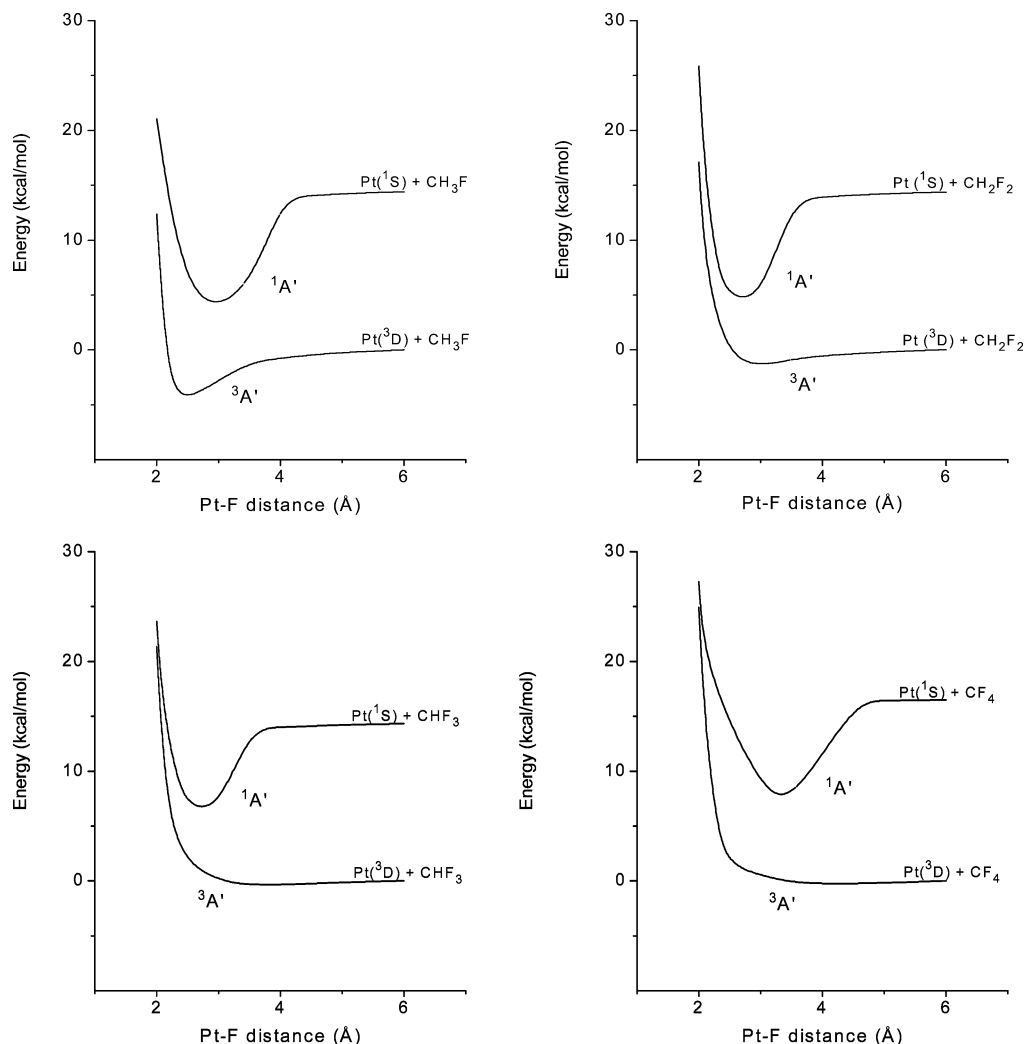


**Figure 1.** Plot of the CASSCF potential energy vs the Pt–F distance for electronic states emerging from the linear approach of the metal to the fluorine atom. The C–F–Pt angle was kept fixed at  $180^\circ$ . Energies are relative to the corresponding ground-state dissociation limit.

For the reaction  $\text{Pt} + \text{CH}_2\text{F}_2$ , the low-lying states belonging to the  $C_1$  symmetry group which evolve from insertion of the metal atom into the C–H bond contained in the F–C–H plane were also investigated. Unlike the equivalent  $C_s$  electronic states, for which the platinum atom lies in the plane containing the two hydrogen atoms, for the less symmetric  $C_1$  states a fluorine atom is next to the C–H bond attacked by the metallic center. Due to limitations in the number of geometrical parameters imposed by the (nongradient) geometry optimization algorithm used, potential-energy curves for states belonging to this symmetry group were calculated constraining the platinum atom to lie in the F–C–H plane. As discussed later, comparison of the results obtained for the states evolving from both reaction geometries allows analyses of the role played by the hydrogen or fluorine atoms next to the C–H bond on the metallic insertion reaction.

For the reaction  $\text{Pt} + \text{CH}_3\text{F}$ , CASSCF calculations were performed taking into account a full valence active space consisting of 24 electrons in 13 orbitals. For the remaining interactions CASSCF potential-energy curves were calculated using an active space consisting of 16 electrons in 10 orbitals. The dimension of the active space was kept fixed throughout all calculations on the different potential-energy curves and included in all cases the s orbital and the six Cartesian d orbitals of platinum. For C–F bond activation reactions the active space also included the three p-type functions of the fluorine atom,

whereas for reactions involving insertion of the metal atom into the C–H bond the s-type functions of the hydrogen and carbon atoms were used in the active space (besides a p function of a fluorine atom).

To improve the evaluation of the energetics of the different reactions investigated, MRMP2 calculations were performed at selected points of each of the CASSCF potential-energy surfaces. In these MRMP2 calculations the CASSCF active orbitals were used as the active space.

For the platinum atom the AREP (averaged relativistic effective potential) and triple- $\zeta$  quality Gaussian basis set for the 5d and 6s shells as given by Ross et al.<sup>20</sup> were used. For consistency, the carbon and fluorine atoms were taken into account using the AREP and triple- $\zeta$  quality basis set for the 2s and 2p valence region subshells developed by Pacios and co-workers.<sup>21,22</sup> Hydrogen atoms were described through the standard 6-31++G\*\* basis set.<sup>23–26</sup>

All calculations were performed using the quantum chemistry code GAMESS.<sup>27</sup>

### 3. Results and Discussion

**a. Linear Pt–F Approach.** Figure 1 shows the CASSCF potential-energy curves for the states arising from the direct Pt–F approach (i.e., that for which the C–F–Pt angle is kept fixed at  $180^\circ$ ) for the different  $\text{Pt} + \text{CH}_{4-n}\text{F}_n$  ( $n = 1–4$ )

**TABLE 1: CASSCF and MRMP2 Energies (kcal/mol) as Well as Some Geometrical Parameters (Å) for the Linear Electronic States Which Evolve from the Direct Approach of the Platinum to the Fluorine Atom (each energy is relative to the ground-state dissociation limit Pt(<sup>3</sup>D;<sub>5d</sub><sup>9</sup>6s<sup>1</sup>) + CH<sub>4–n</sub>F<sub>n</sub>)**

$\angle\text{C-Pt-F} = 180^\circ$	state	energy		distance	
		CASSCF	MRMP2	Pt–F	C–F
Pt + CH <sub>3</sub> F	<sup>3</sup> A'	–4.49	–7.44	2.41	1.48
Pt + CH <sub>3</sub> F	<sup>1</sup> A'	4.57	–11.90	2.43	1.48
Pt + CH <sub>2</sub> F <sub>2</sub>	<sup>3</sup> A'	–2.21	–3.38	2.50	1.45
Pt + CH <sub>2</sub> F <sub>2</sub>	<sup>1</sup> A'	4.98	–7.66	2.45	1.45
Pt + CHF <sub>3</sub>	<sup>3</sup> A'	–0.35	–0.74	3.16	1.38
Pt + CHF <sub>3</sub>	<sup>1</sup> A'	6.78	–7.18	2.60	1.41
Pt + CF <sub>4</sub>	<sup>3</sup> A'	–0.25	0.27	2.85	1.39
Pt + CF <sub>4</sub>	<sup>1</sup> A'	8.08	–2.08	3.50	1.38

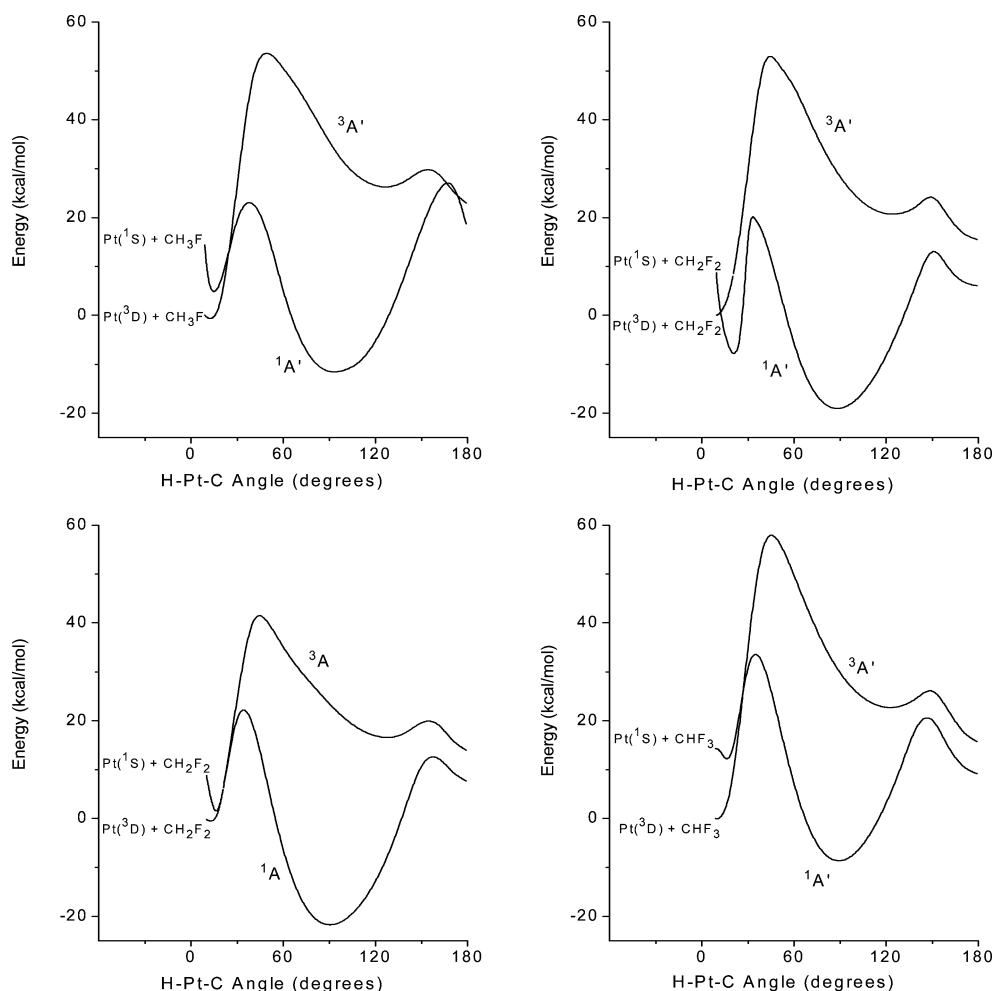
reactions. Values for the energy minima appearing in this figure are shown in Table 1. Energies evolving from MRMP2 single-point calculations at these minima are also provided in this table. Whereas only small variations in the energy of the triplet states are obtained after inclusion of dynamical electron correlation effects, singlet states emerging from the first excited asymptotic limit are significantly stabilized at the MRMP2 level. Similar trends have been previously reported by Nakao et al.<sup>28</sup> for the triplet and singlet states evolving from the reactions M<sup>+</sup> (Sc, Ni, Cu) + NH<sub>3</sub>.

Although exhibiting energy minima slightly less deep than their corresponding low-multiplicity channels, triplet states

arising from the Pt + CH<sub>3</sub>F and Pt + CH<sub>2</sub>F<sub>2</sub> ground-state asymptotes are also stable. For both multiplicity channels stability of the adducts decreases as the number of fluorine atoms increases in the fluorocarbon compound (the PtCF<sub>4</sub> singlet state lying only 2 kcal/mol below the ground-state asymptotic limit). No significant variation in the C–F distance (relative to the equilibrium distance at the corresponding isolated molecule) is predicted for states evolving from this approaching mode, so they do not represent viable channels for activation of this bond by the platinum atom.

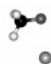
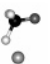



**b. Pt Insertion into the C–H Bond.** As shown in Figure 2, oxidative addition of the C–H bond of the different fluorocarbon compounds to the platinum atom could be exothermic only through reaction channels involving the singlet state correlating with the first excited asymptotic limit Pt(<sup>1</sup>S;<sub>5d</sub><sup>10</sup>) + CH<sub>4–n</sub>F<sub>n</sub> ( $n = 1–3$ ) as the triplet potential-energy curves evolving from the ground state of the reactants are all repulsive. As previously discussed by Carroll et al.<sup>7</sup> for the similar reaction Pt + CH<sub>4</sub>, a curve crossing to the singlet state must occur in each case so reaction could take place from the ground state of the free fragments.

A potential-energy well lying below the energy of the corresponding ground-state asymptotic limit was determined for each of the low-multiplicity channels at H–Pt–C angles near 90°. For each of these states the main configuration state function at the energy minimum corresponds to a closed-shell occupancy. Energy values and geometrical parameters for the



**Figure 2.** CASSCF potential-energy curves for the low-lying electronic states evolving from metal insertion into the C–H bond of the molecules CH<sub>4–n</sub>F<sub>n</sub> ( $n = 1–3$ ). For the Pt + CH<sub>2</sub>F<sub>2</sub> reaction plots for states belonging to both C<sub>s</sub> and C<sub>1</sub> symmetry groups are shown. Energies are relative to the corresponding ground-state dissociation limit.

**TABLE 2: MRMP2 Energies (kcal/mol) for the Singlet States Evolving from Insertion of Platinum into the C–H Bond<sup>a</sup>**

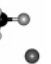
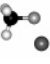
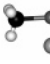
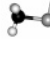
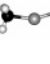
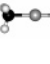
	State	Local energy minimum	TS1	Energy minimum	TS2	C–Pt–H structure (180°)
						
Pt + CH <sub>3</sub> F	<sup>1</sup> A'	-9.62	2.73	-36.27	16.36	9.36
Pt + CH <sub>2</sub> F <sub>2</sub> (C <sub>s</sub> )	<sup>1</sup> A'	-	3.38	-36.94	-0.24	1.94
Pt + CH <sub>2</sub> F <sub>2</sub> (C <sub>1</sub> )	<sup>1</sup> A	-8.71	8.46	-40.17	10.22	6.11
Pt + CHF <sub>3</sub>	<sup>1</sup> A'	-8.47	9.79	-42.65	7.41	-5.80

<sup>a</sup>Energies are relative to the ground-state dissociation limit Pt(<sup>3</sup>D;5d<sup>9</sup>6s<sup>1</sup>) + CH<sub>4-n</sub>F<sub>n</sub>.

**TABLE 3: Geometrical Parameters (deg and Å) Corresponding to the Low-Lying Electronic States Which Evolve from Insertion of Platinum into the C–H Bond of Each of the Molecular Fragments**

	state	H–Pt–C angle	distance		
			Pt–H	Pt–C	C–H
PtCH <sub>3</sub> F	<sup>1</sup> A'	91.0	1.51	1.98	2.51
PtCH <sub>2</sub> F <sub>2</sub> (C <sub>s</sub> )	<sup>1</sup> A'	86.7	1.52	1.98	2.43
PtCH <sub>2</sub> F <sub>2</sub> (C <sub>1</sub> )	<sup>1</sup> A	90.2	1.53	1.96	2.49
PtCHF <sub>3</sub>	<sup>1</sup> A'	88.1	1.52	1.95	2.43

**TABLE 4: MRMP2 Energies (kcal/mol) for the Singlet States Evolving from Insertion of Platinum into the C–F Bond<sup>a</sup>**

	Local energy minimum	TS1	PtF + CH <sub>4-n</sub> F <sub>n-1</sub> asymptote	Energy minimum	TS2	C–Pt–F structure (180°)
						
Pt + CH <sub>3</sub> F	-10.24	8.14	16.6	-45.82	-37.51	-40.65
Pt + CH <sub>2</sub> F <sub>2</sub>	-11.38	8.74	15.8	-52.15	-41.09	-39.79
Pt + CHF <sub>3</sub>	-11.13	18.50	22.5	-41.46	-38.80	-42.42
Pt + CF <sub>4</sub>	-9.63	23.68	16.4	-52.16	-28.43	-28.17

<sup>a</sup>Energies are relative to the ground-state dissociation limit Pt(<sup>3</sup>D;5d<sup>9</sup>6s<sup>1</sup>) + CH<sub>4-n</sub>F<sub>n</sub>.

oxidative addition products are provided in Tables 2 and 3, respectively. The significant C–H elongation distance obtained for the different insertion products (which in each case is more than twice the C–H equilibrium distance at the isolated fluorocarbon molecule) indicates that the C–H bond activation by platinum is feasible for all interactions. For neither of these insertion reactions has any significant elongation of the C–H or C–F bonds nearest the C–H bond being activated by the metallic atom been detected; therefore, our results do not support the possibility of a mechanism involving a double C–H bond activation (or a C–H and C–F simultaneous bond activation) for these reactions, such as that determined by Carroll et al.<sup>7</sup> for the Pt + CH<sub>4</sub> reaction.

Although a stable C–Pt–H linear structure is predicted for the PtCHF<sub>3</sub> singlet state, a considerable energy barrier (roughly 50 kcal/mol) prevents reaching this structure. For the Pt + CH<sub>3</sub>F reaction the energy value at the second barrier is practically the same as that corresponding to the asymptotic limit PtF + CH<sub>3</sub> (shown in Table 4), thus suggesting for this reaction channel formation of the methyl radical as a possible product under high-temperature conditions. A similar result has been reported by Hwang et al.<sup>6</sup> for the PtO + CH<sub>4</sub> reaction.

Singlet states emerging from the C–H bond activation reaction taking place in the F–C–H plane of the different fluorinated fragments exhibit a similar pattern at the first stage of the reaction (in fact, with exception of the singlet state

evolving from the C<sub>s</sub> approach of the reactants Pt + CH<sub>2</sub>F<sub>2</sub>, the remaining states fall into this category). For these states the local energy minimum appearing at the potential-energy curve as the reactants approach each other indicates formation of a molecular precursor (Figure 2). As seen from Table 2, energy values at these local potential-energy wells do not vary significantly with the number of fluorine atoms in the molecular fragment. Instead, the attractive character at small H–Pt–C angles seems to be related to interactions arising between the s metallic orbital and the p-type functions of the fluorine atom lying in the plane of the metallic attack, which slightly stabilize the σ(p<sub>C</sub> – p<sub>F</sub>) molecular orbital. It is important to point out that these weak interactions, favoring stabilization of the molecular precursors, contribute significantly to increase the energy barrier along reaction paths involving these pre-reaction complexes. Thus, whereas the height of the energy barrier for the Pt + CH<sub>3</sub>F reaction is only 2.7 kcal/mol relative to the ground-state dissociation limit (this value is similar to that reported by Carroll et al.<sup>7</sup> for the C–H bond activation in methane by platinum), the calculated barrier for the reaction taking place from the molecular precursor is 12.3 kcal/mol. Slightly higher energy barriers (relative to the ground-state asymptote) are obtained for the Pt + CH<sub>2</sub>F<sub>2</sub> (C<sub>1</sub>) and Pt + CHF<sub>3</sub> reactions, 8.46 and 9.79 kcal/mol, respectively. As seen from Table 2, the barriers which must be surmounted when these reactions occur via stabilization of the molecular precursor are nearly twice these values.

The singlet state arising from metal insertion into a C–H bond of the CH<sub>2</sub>F<sub>2</sub> molecule for the reaction taking place in the H–C–H plane of the fluorinated molecule (C<sub>s</sub> symmetry) exhibits a different behavior. Although the CASSCF potential-energy curve (Figure 2) for this state looks similar to those previously discussed for the remaining singlet states, energy results obtained at the MRMP2 level significantly change the shape of this curve as the potential-energy well appearing at the initial stage of the curve is removed and the height of the energy barrier is significantly decreased after inclusion of the electron correlation (Table 2). The main configuration state function at this region resembles the d<sup>10</sup> electronic configuration of the first excited-state asymptotic limit (in contrast with the d<sup>9</sup>s<sup>1</sup> type configuration in the metallic fragment at the local energy minima for the remaining singlet states). For this state only negligible s-type orbital interactions between the platinum and hydrogen atoms were detected (consistent with the maximal d-shell occupancy configuration). Insertion of the metallic atom into the C–H bond through this channel occurs therefore without formation of a pre-reaction complex. Instead, this low-multiplicity curve crosses the triplet potential-energy curve roughly 4.1 kcal/mol above the ground state of the reactants. As for the Pt + CH<sub>4</sub> reaction,<sup>7</sup> this crossing-point energy can be proposed as the activation energy for this reaction channel. According to energy data in Table 2, the energy barrier for the C–H bond activation reaction in the CH<sub>2</sub>F<sub>2</sub> molecule when insertion of the metal takes place in the H–C–H plane is 13 kcal/mol below the corresponding value for the reaction occurring in the F–C–H plane via stabilization of the molecular precursor (as for the C<sub>1</sub> singlet state the metallic atom was constrained to lie in the F–C–H plane reaction paths leading from the C<sub>1</sub> channel to the more favorable C<sub>s</sub> one were not investigated). A similar behavior (a barrierless insertion) has been determined by Smurnyi et al.<sup>8</sup> for Pt + CH<sub>3</sub>F reaction when metal insertion takes place in the H–C–H plane far away from the fluorine atom. Thus, from this comparison the height of the energy barriers for these kinds of reactions depends importantly on

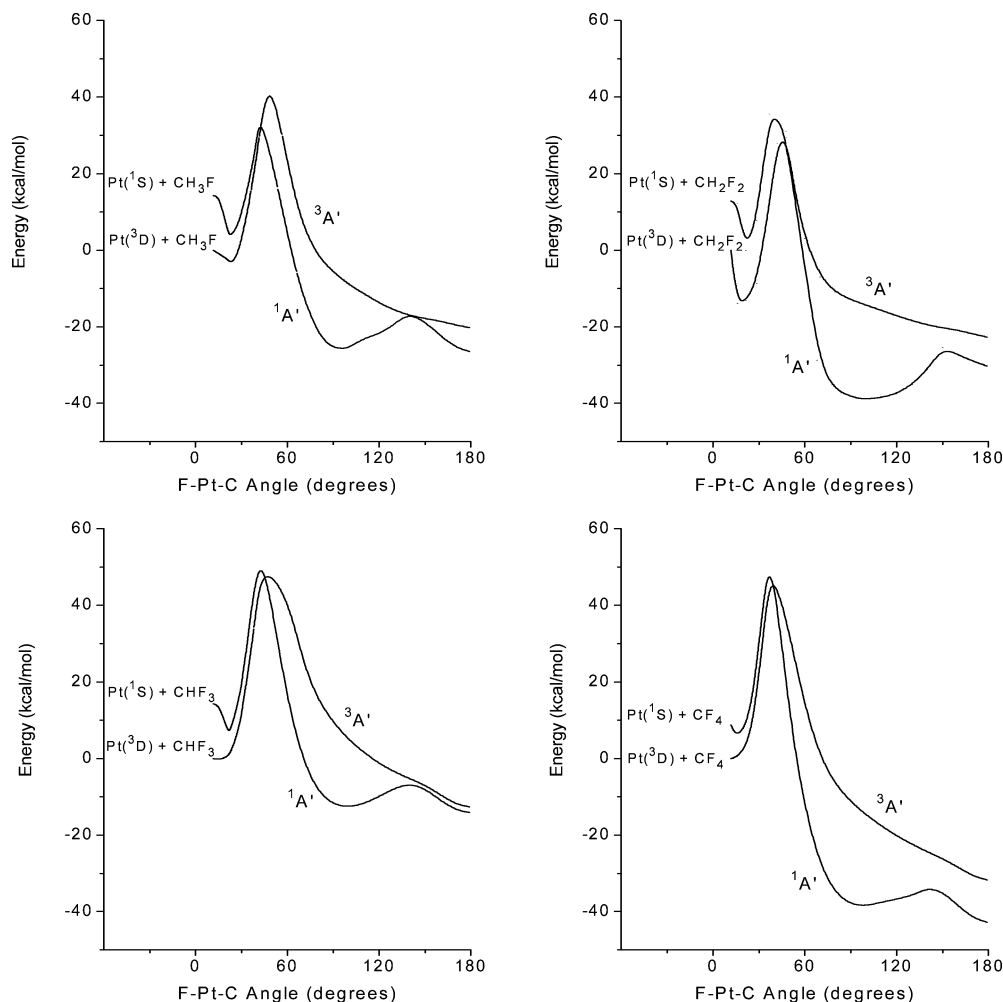


**Figure 3.** CASSCF potential-energy curves for the electronic states arising from insertion of the platinum atom into the C–F bond of the different fluorocarbon compounds. Energies are relative to the corresponding ground-state dissociation limit.

interactions arising between the metallic atom and the hydrogen or fluorine atom next to the C–H bond being activated (i.e., lying in the C–Pt–H insertion plane).

**c. Pt Insertion into the C–F Bond.** The CASSCF potential-energy curves associated with the low-lying electronic states which arise from insertion of the platinum atom into the C–F bond of the CH<sub>4–n</sub>F<sub>n</sub> molecules are shown in Figure 3. Although the reaction energy for oxidative addition of the different fluorocarbon compounds to the platinum atom is favorable for both multiplicity channels, reaction along the singlet potential curve evolving from the first excited asymptote always leads to the deepest energy minimum. A crossing between the triplet and singlet potential-energy curves must occur in each case so the reaction path leading to the most stable product takes place from the ground state of the free fragments. In the same way as for the C–H bond activation reactions discussed before, the main features of the C–F bond activation process in these kinds of systems are strongly determined by the potential-energy curve correlating with the first excited dissociation limit Pt(1S;5d<sup>10</sup>) + CH<sub>4–n</sub>F<sub>n</sub>.

Interestingly, this reaction pattern, which involves an important participation of the maximal d-shell occupancy metallic state, resembles those previously determined for other simple interactions between small molecules and transition-metal atoms.<sup>29,30</sup> MRMP2 energies calculated at the stationary points of the low-multiplicity potential curves are provided in Table 4. Some geometrical parameters at the energy minima for these states appear in Table 5.

**TABLE 5: Geometrical Parameters (deg and Å) Corresponding to the Low-Lying Electronic States Which Evolve from Insertion of Platinum into the C–F Bond of Each of the Molecular Fragments**

	state	F–Pt–C angle	distance		
			Pt–F	Pt–C	C–F
PtCH <sub>3</sub> F	<sup>1</sup> A'	96.2	1.97	2.02	2.98
PtCH <sub>2</sub> F <sub>2</sub>	<sup>1</sup> A'	116.2	1.99	1.95	3.35
PtCHF <sub>3</sub>	<sup>1</sup> A'	103.1	2.00	1.95	3.09
PtCF <sub>4</sub>	<sup>1</sup> A'	104.7	1.99	1.92	3.11

A bent structure with a C–Pt–F angle varying between 96° and 116° is predicted for most of the oxidative addition products. For the Pt + CHF<sub>3</sub> reaction the bent and linear structures are both possible for the oxidative addition product as a very low-energy barrier (2.6 kcal/mol) separates the potential-energy wells corresponding to these geometrical arrangements (interestingly, structures with a linear C–Pt–F angle are obtained for the less stable insertion products evolving from the high multiplicity channels).

As seen in Table 5, the predicted structure for the different insertion products involves in all cases a significant C–F bond distance elongation relative to the equilibrium value at the corresponding isolated fluorocarbon compound (calculated values for this distance in the different fluorinated molecules fall within the 1.34–1.46 Å range). As expected, C–F interaction at the region of the energy minima diminishes significantly. Instead, Pt–C and Pt–F molecular interactions involving the p-type functions of carbon and fluorine atoms and the metallic

d orbitals appear at these potential-energy wells. The slightly greater stabilization calculated for products of Pt + CH<sub>2</sub>F<sub>2</sub> and Pt + CF<sub>4</sub> reactions arises from molecular interactions involving the fluorine atom next to the C–F bond being activated, as reflected by a slight increase of the C–F distance involving this second fluorine atom (roughly 5% of the C–F calculated distance at the isolated fluorocarbon fragments).

Weak interactions between the metallic s orbital and the p-type functions of the fluorine atom arise as reactants approach each other along the low-multiplicity reaction paths, favoring in each case stabilization of a molecular precursor (this is also true for the triplet states arising from insertion of the metal into the C–F bond of the CH<sub>3</sub>F and CH<sub>2</sub>F<sub>2</sub> molecules). Stabilization of a prereaction complex at an early stage of the Pt + CHF<sub>3</sub> reaction has also been reported by Smurnyi et al.<sup>8</sup>

Unlike C–H bond activation reactions in the CH<sub>4–n</sub>F<sub>n</sub> (*n* = 1–3) molecules, for which these metal–halogen attractive interactions arise only along those reactions paths involving a fluorine atom lying in the C–Pt–H insertion plane, interactions appearing at the early stage of the C–F bond activation reactions are inherent to all these reaction systems as they involve the fluorine atom participating in the C–F bond being activated. Whereas these interactions do not give rise to significant changes in the geometry of the fluorinated fragments, they contribute to increase the energy barrier of reactions occurring via stabilization of the molecular precursor. As seen from the energy data in Table 4, for the Pt + CH<sub>3</sub>F reaction the height of the energy barrier relative to the ground-state dissociation limit is 8.14 kcal/mol, but a barrier near 18.3 kcal/mol must be surmounted before the oxidative addition product could be reached through the reaction path involving the prereaction complex. For the remaining reactions in Table 4 the height of the energy barriers relative to the ground-state asymptote increases as the number of fluorine atoms present in the fluorocarbon compound, in the same direction as the strength of the C–F bond increases (as reflected by the shortening in the calculated C–F bond distance from CH<sub>3</sub>F to CF<sub>4</sub> in the isolated molecules). In all cases the barrier for reactions taking place through the molecular precursor is increased by roughly the same amount that is found for the Pt + CH<sub>3</sub>F reaction.

Calculations near the transition-state region (TS1) of the different C–F bond activation reactions allowed detecting the asymptotic limit CH<sub>4–n</sub>F<sub>n–1</sub> (*n* = 1–4) + Pt–F involving radical species. As shown in Table 4, this asymptote lies above the transition-state energy for most of the low-multiplicity states; thus, occurrence of this dissociated state does not affect conclusions drawn before on these reaction channels. However, for the Pt + CF<sub>4</sub> interaction the asymptotic limit CF<sub>3</sub> + Pt–F lies below the transition-state energy associated with both multiplicity reaction channels Pt(<sup>3</sup>D, <sup>1</sup>S) + CF<sub>4</sub>, thus suggesting that C–F breaking and Pt–F bond formation could occur before the oxidative addition product is reached. This preference toward the radical products could be related to the great stability of the radical CF<sub>3</sub>.<sup>11</sup> The transition-state energy for most of the triplet channels lies above the Pt–F + CH<sub>4–n</sub>F<sub>n–1</sub> limit, indicating that for reactions taking place along the high-multiplicity path the radical products are also preferred over the oxidative addition product.

**d. Comparison between C–H and C–F Insertion Reactions.** Whereas reaction channels leading to stable products are predicted for insertion of the platinum atom into both the C–H and the C–F bonds of the CHF<sub>3</sub>, CH<sub>2</sub>F<sub>2</sub> and CHF<sub>3</sub> compounds (Tables 2 and 4), oxidative addition of C–F to the metallic atom

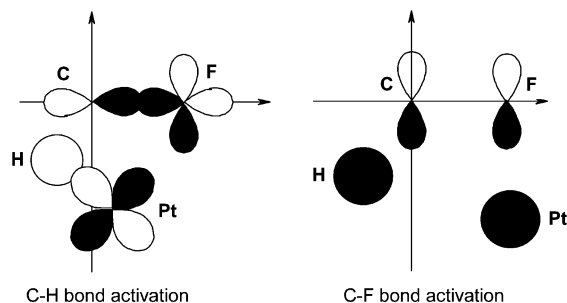
leads in most cases to the more stable insertion product (stability of C–H and C–F insertion products evolving from Pt + CHF<sub>3</sub> reactants is nearly the same). Kinetic preferences follow the opposite trend as the calculated energy barrier for insertion of the metal atom into the C–F bond of the different fluorocarbon compounds is greater than the corresponding C–H reaction. As seen in Tables 2 and 4, the height of the energy barrier for each of the C–F bond activation reactions is more than twice the corresponding value of the C–H reaction, thus suggesting a kinetic preference for the oxidative addition of the C–H bond into the platinum atom. Opposite thermodynamic and kinetic trends for the C–H and C–F bond activation reactions have been reported by Smurnyi et al.<sup>8</sup> for the Pt + CH<sub>3</sub>F reaction.

As stable products can be reached for insertion of the metallic atom into both the C–H and the C–F bonds of the different hydrogenated fluorocarbon compounds, kinetic factors must play an important role in determining the competition between C–H and C–F bond activation in these reaction systems.

In accord with the results discussed in the previous sections, metal–halogen interactions arising at the early stage of all C–F activation reactions and most of the C–H reactions contribute to increase the height of the energy barrier for these reactions (a similar stabilization energy is associated with the molecular precursors arising from the low-multiplicity channels of both activation reactions). On the other hand, reactions Pt + CH<sub>3</sub>F and Pt + CH<sub>2</sub>F<sub>2</sub> can take place in the H–C–H plane, far away from the fluorine atom. Features of the potential curves for these reaction channels are similar to those previously determined for insertion of platinum into the C–H bond of methane, namely, a very small activation energy or even barrierless insertion of the metal into the C–H bond.<sup>7,8</sup> The existence of these reaction channels favors markedly C–H bond activation over the corresponding C–F reaction. For the reaction Pt + CH<sub>2</sub>F<sub>2</sub> the height of the energy barrier for insertion of the platinum atom into the C–F bond through the singlet reaction channel is 20 kcal/mol when reaction occurs via stabilization of the molecular precursor. Although this value is similar to that corresponding to C–H bond activation in the same molecule through the C<sub>1</sub> low-multiplicity reaction channel (17.1 kcal/mol), C–H bond activation will be preferred as metal insertion into the C–H bond through the singlet channel belonging to the C<sub>s</sub> symmetry group, which takes place far away from the fluorine atom, proceeds with a significantly small energy barrier (3.3 kcal/mol).

Additional information that could be helpful to explain differences among the height of the energy barriers calculated for C–H and C–F insertion reactions can be obtained from molecular orbital analysis at different regions of the potential-energy curves. In accord with data evolving from this analysis at the energy minima, d-type metallic functions contribute significantly to stabilize the insertion products emerging from both the C–H and the C–F bond activation reactions. Interestingly, molecular orbital analysis carried out at insertion angles near the energy barriers of the C–H bond activation reactions indicates that d-type metallic orbitals are already important at this region as being responsible for transferring charge into the σ\*(C–H) as well as contributing to form bonding interactions with the hydrogen and carbon atoms (Scheme 2). For C–F bond activation reactions participation of d-type functions at the same region is only marginal and the main metal–molecule interactions involve only the s metallic orbital. Thus, the weakening of the C–F bond reached at the energy barrier along these reaction paths is not compensated yet by bonding interactions between the carbon and fluorine atoms and the metallic d-type

## SCHEME 2



orbitals. In this sense, aspects emerging from comparison of the potential-energy curves at the initial stage of the C–H and C–F bond activation reactions, such as the earlier occurrence (at small insertion angles) and the lower height of the energy barriers for the former, could be explained in terms of the earlier participation of the metallic d orbitals in the C–H insertion reactions relative to the corresponding C–F bond activation reactions.

## 4. Conclusions

Potential-energy curves for the low-lying triplet and singlet electronic states evolving from the Pt + CH<sub>4–n</sub>F<sub>n</sub> ( $n = 1–4$ ) interactions were determined for different approaching modes of the reactants. Stable states involving an important C–H or C–F bond elongation were detected only for insertion of the metallic atom into the C–H and C–F bonds of the different fluorocarbon compounds. Comparison of the calculated values of the energy barrier for these reactions in the different fluorocarbon compounds suggests in all the cases a kinetic preference for the C–H bond activation reaction.

Factors such as stabilization of molecular precursors arising as a consequence of metal–halogen interactions at the early stage of the C–F bond activation reactions as well as lack of bonding molecular orbitals involving d-type metallic contributions at the energy barriers appearing at the potential-energy curves for the C–F insertion reactions could play an important role in determining the kinetic preference toward the C–H bond activation in these reaction systems.

**Acknowledgment.** This research was partially supported by the Universidad Nacional Autónoma de México (DGAPA-IN119305) and El Consejo Nacional de Ciencia y Tecnología (CONACyT-44494-Q).

## References and Notes

(1) Zaric, S.; Hall, M. B. *J. Phys. Chem. A* **1997**, *101*, 4646 and references therein.

- (2) Dedieu, A. *Chem. Rev.* **2000**, *100*, 572 and references therein.  
 (3) Wittborn, A. M. C.; Costas, M.; Blomberg, M. R. A.; Siegbahn, P. E. M. *J. Chem. Phys.* **1997**, *107*, 4318.  
 (4) Cui, Q.; Musaev, D. G.; Morokuma, K. *J. Chem. Phys.* **1998**, *108*, 8418.  
 (5) Achatz, U.; Beyer, M.; Joos, S.; Fox, B. S.; Niedner-Schatteburg, G.; Bondybey, V. E. *J. Phys. Chem. A* **1999**, *103*, 8200.  
 (6) Hwang, D.; Mebel, A. M. *Chem. Phys. Lett.* **2002**, *365*, 140.  
 (7) Carroll, J. J.; Weisshaar, J. C.; Siegbahn, P. E. M.; Wittborn, C. A. M.; Blomberg, M. R. A. *J. Phys. Chem.* **1995**, *99*, 14388.  
 (8) Smurnyi, E. D.; Gloriovov, I. P.; Ustynyuk, Y. A. *Russ. J. Phys. Chem.* **2003**, *77*, 1699.  
 (9) Kiplinger, J. L.; Richmond, T. G.; Osterberg, C. E. *Chem. Rev.* **1994**, *94*, 373.  
 (10) Su, M.; Chu, S. *J. Am. Chem. Soc.* **1997**, *119*, 10178.  
 (11) Chen, Q.; Freiser, B. S. *J. Phys. Chem. A* **1998**, *102*, 3343.  
 (12) Bosque, R.; Clot, E.; Fantacci, S.; Maseras, F.; Eisenstein, O.; Perutz, R. N.; Renkema, K. B.; Caulton, K. G. *J. Am. Chem. Soc.* **1998**, *120*, 12634.  
 (13) Jakt, M.; Johannissen, L.; Rzepa, H. S.; Widdowson, D. A.; Wilhelm, R. *J. Chem. Soc., Perkin Trans.* **2002**, 576.  
 (14) Gerard, H.; Davidson, E. R.; Eisenstein, O. *Mol. Phys.* **2002**, *100*, 533.  
 (15) Reinhold, M.; McGrady, J. E.; Perutz, R. N. *J. Am. Chem. Soc.* **2004**, *126*, 5268.  
 (16) Kiplinger, J. L.; King, M. A.; Arif, A. M.; Richmond, T. G. *Organometallics* **1993**, *12*, 3382.  
 (17) Crespo, M.; Martinez, M.; de Pablo, E. *J. Chem. Soc., Dalton Trans.* **1997**, 1231.  
 (18) Villanueva, L.; Bernès, S.; Torrens, H. *Chem. Commun.* **2004**, 1942.  
 (19) Richmond, T. G. *Topics in Organometallic Chemistry*; Murai, S., Ed.; Springer-Verlag: Berlin, 1999; p 244.  
 (20) Ross, R. B.; Powers, J. M.; Atashroo, T.; Ermler, W. C.; LaJohn, L. A.; Christiansen, P. A. *J. Chem. Phys.* **1990**, *93*, 6654.  
 (21) Pacios, L. F.; Gómez, P. C. *Int. J. Quantum Chem.* **1994**, *49*, 817.  
 (22) Pacios, L. F.; Christiansen, P. A. *J. Chem. Phys.* **1985**, *82*, 2664.  
 (23) Hehre, W. J.; Ditchfield, R.; Pople, J. A. *J. Chem. Phys.* **1972**, *56*, 2257.  
 (24) Hariharan, P. C.; Pople, J. A. *Theor. Chim. Acta* **1973**, *28*, 213.  
 (25) Clark, T.; Chandrasekhar, J.; Schleyer, P. V. R. *J. Comput. Chem.* **1983**, *4*, 294.  
 (26) Basis set was obtained from the Extensible Computational Chemistry Environment Basis Set Database, Version 02/25/04, as developed and distributed by the Molecular Science Computing Facility, Environmental and Molecular Sciences Laboratory, which is part of the Pacific Northwest Laboratory, P.O. Box 999, Richland, WA 99352, and funded by the U.S. Department of Energy. The Pacific Northwest Laboratory is a multiprogram laboratory operated by Battelle Memorial Institute for the U.S. Department of Energy under contract DE-AC06-76RLO 1830. Contact Karen Schuchardt for further information.  
 (27) Schmidt, M. W.; Baldrige, K. K.; Boatz, J. A.; Elbert, S. T.; Gordon, M. S.; Jensen, J. H.; Koseki, S.; Matsunaga, N.; Nguyen, K. A.; Su, S. J.; Windus, T. L.; Dupuis, M.; Montgomery, J. A. *J. Comput. Chem.* **1993**, *14*, 1347.  
 (28) Nakao, Y.; Taketsugu, T.; Hirao, K. *J. Chem. Phys.* **1999**, *110*, 10863.  
 (29) Colmenares, F.; Ramírez-Solís, A.; Novaro, O. *Chem. Phys. Lett.* **2001**, *345*, 111.  
 (30) Colmenares, F.; Meléndez, S. *Chem. Phys. Lett.* **2003**, *380*, 292.